Protective Transfer: Maternal passive immunization with a rotavirus-neutralizing dimeric IgA protects against rotavirus disease in suckling neonates

Langel SN[1,2], Steppe JT[3], Chang J[3], Travieso T[3], Webster H[3], Otero CE[3,4], Williamson LE[5,6,7], Crowe JE Jr[5,6,7], Greenberg HB[8], Wu H[9], Hornik C[9,10], Mansouri K[3], Edwards RJ[3,11], Stalls V[3], Acharya P[2,3], Blasi M[3,11*], Permar SR[12*]

[1]Duke Center for Human Systems Immunology, Durham, NC, USA

[2]Department of Surgery, Duke University School of Medicine, Durham, NC, USA

[3]Duke Human Vaccine Institute, Duke University School of Medicine, Durham, NC, USA

[4]Department of Pathology, Duke University School of Medicine, Durham, NC, USA

[5]Vanderbilt Vaccine Center, Vanderbilt University Medical Center, Nashville, TN, USA

[6]Department of Pathology, Microbiology and Immunology, Vanderbilt University Medical Center, Nashville, TN, USA

[7]Department of Pediatrics, Vanderbilt University Medical Center, Vanderbilt, TN, USA

[8]Departments of Medicine and Microbiology and Immunology, Stanford University School of Medicine, Stanford CA, USA. and the VA Palo Alto Health Care System, Department of Veterans Affairs, Palo Alto, CA, USA

[9]Department of Pediatrics, Duke University School of Medicine, Durham, NC, USA

[10]Duke Clinical Research Institute, Duke University School of Medicine, Durham, NC, USA

[11]Department of Medicine, Duke University School of Medicine, Durham, NC, USA

[12]Department of Pediatrics, Weill Cornell Medical College, NYC, NY USA

*Correspondence should be addressed to: Maria Blasi, Duke University Medical Center, 2 Genome Ct, 27710 Durham, NC, USA. E-mail: maria.blasi@duke.edu and Sallie Permar, Weill Cornell Medicine/NewYork Presbyterian Hospital E-mail: sallie.permar@med.cornell.edu

29 **GRAPHICAL ABSTRACT**

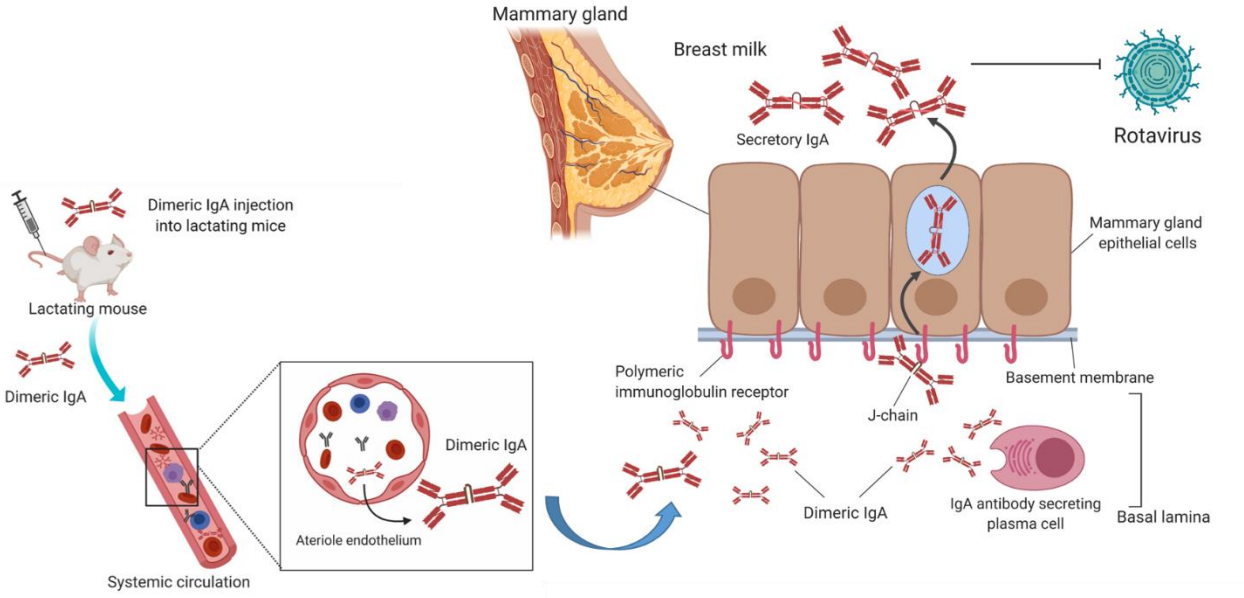

30

SUMMARY

Breast milk secretory IgA antibodies provide a first line of defense against enteric infections. Despite this and an effective vaccine, human rotaviruses (RVs) remain the leading cause of severe infectious diarrhea in children in low- and middle-income countries (LMIC) where vaccine efficacy is lower than that of developed nations. Therapeutic strategies that deliver potently neutralizing antibodies into milk could provide protection against enteric pathogens such as RVs. We developed a murine model of maternal protective-transfer using systemic administration of a dimeric IgA (dIgA) monoclonal antibody. We confirmed that systemically-administered dIgA passively transferred into milk and stomach of suckling pups in a dose-dependent manner. We then demonstrated that systemic administration of an engineered potent RV-neutralizing dIgA (mAb41) in lactating dams protected suckling pups from RV-induced diarrhea. This maternal protective-transfer immunization platform could be an effective strategy to improve infant mortality against enteric infections, particularly in LMIC with high rates of breastfeeding.

INTRODUCTION

Rotavirus (RV), a common enteric pathogen, is responsible for ~125,000-215,000 deaths in children <5 years and is the leading cause of gastroenteris-related hospitalizations worldwide, particularly in low and middle-income countries (LMIC) (Burke et al., 2019). While oral live, attenuated RV vaccines have significantly reduced RV-associated disease and death worldwide (Burnett et al., 2017), RV vaccines demonstrate lower efficacy in children in LMIC (40-60%) compared to those in high-income countries (80-90%) (Jonesteller et al., 2017; Mwila et al., 2017). The combination of decreased RV vaccine efficacy, high rates of RV exposure and an immature immune system creates a 'window of susceptibility' when infants and toddlers are particularly vulnerable. Strategies to provide additional antibody-mediated protection are needed to narrow this critical window of vulnerability and further decrease RV-associated disease and death.

While maternal immunization could be employed as a strategy to boost protective antibodies in breast milk, pregnant women in areas with high RV-associated morbidity and mortality experience undernutrition (Desyibelew and Dadi, 2019), micronutrient deficiencies (Harika et al., 2017) and chronic enteropathies that may impact generation of potently neutralizing anti-RV responses. Indeed, previous studies have demonstrated that socioeconomic status plays a role in generation of anti-RV antibodies (Ray et al., 2007; Trang et al., 2014). Additionally, maternal vaccination may lead to maternal antibody interference and decreased immunogenicity in vaccinated infants (Appaiahgari et al., 2014; Otero et al., 2020). Based on this, other therapeutic strategies for delivery of potently RV-neutralizing antibodies are needed.

In humans and animal models, a high titer of intestinal RV-specific IgA is a correlate of protection against RV infection and illness (Blutt et al., 2012; Matson et al., 1993; Tô et al., 1998). Therefore, an ideal way to increase protection against RV infection is to provide RV-neutralizing IgA to the infant gut via breast milk. Breast milk contains mostly secretory IgA (sIgA) antibodies; proteolytically stable dimers connected by a joining (J) chain (Corthesy, 2013; Hurley and Theil, 2011). Passive transfer of sIgA into breast milk depends on locally-produced dimeric IgA (dIgA) binding to polymeric immunoglobulin receptor (pIgR) on the basal side of mammary gland epithelial cells via the J-chain (Goldblum et al., 1975; Johansen et al., 1999; Tuaillon et al., 2009). The dIgA-pIgR complex is then transferred across mammary gland epithelium and secreted into breast milk as sIgA (De Groot et al., 2000). Once in milk, sIgA provides immune protection by neutralizing enteric toxins and pathogenic microorganisms and mediating microbiota colonization through exclusion of exogenous competitors (Mantis et al., 2011; Pabst and Slack, 2020). In LMIC, high RV-specific antibody titers in breast milk were associated with decreased incidence of infant RV diarrhea, and partial breastfeeding significantly increased the risk of infant mortality due to diarrheal disease compared to exclusive breastfeeding (Arifeen et al., 2001; Jayashree et al., 1988). However, milk RV-neutralizing antibody titers vary greatly in women from LMIC and may not provide adequate levels of protection (Trang et al., 2014). Therefore, developing dIgA therapeutics that are designed for passive transfer into mucosal compartments, including breast milk, is a novel strategy for enhancing protection of the mother-infant dyad against infectious enteric pathogens.

Here, we developed a murine model of maternal systemic passive antibody immunization for transfer into breast milk using a murine dIgA monoclonal antibody (mAb). We demonstrate that following systemic administration of a dIgA mAb in lactating mice, the mAb is rapidly transported into milk and quickly detected in pup stomach content in a dose-dependent manner. We then engineered a murine dIgA version of a human RV-neutralizing IgG (mAb41) (Nair et al., 2017) and optimized it for enhanced production of dIgA antibodies *in vitro*. We show that dams systemically injected with the RV-neutralizing dIgA mAb provided protection to their pups against RV-associated diarrhea. Our results demonstrate that dIgA can passively transfer out of circulation and into milk to provide a novel strategy for protection against RV disease in suckling neonates. These studies support the need for clinical assessment of maternal protective transfer via passive immunization with dIgA, particularly in LMIC where infant enteric disease burden is high.

RESULTS

Maternal systemic administration of dIgA results in antibody transfer into milk of lactating mice and the gastrointestinal tract of their pups.

To determine whether systemically-administered dIgA passively transfers into milk, we first used a dIgA mAb generated from a previously-described non-neutralizing RV-specific murine dIgA 7D9 hybridoma cell line (Burns et al., 1996). We confirmed 7D9 dIgA binding to cognate antigen, the RV capsid protein VP6, and the J-chain receptor pIgR (Figure 1A) demonstrating that 7D9 contains the J-chain needed for pIgR-mediated passive transfer into milk (Figure 1A). The purified 7D9 hybridoma

supernatant was also confirmed to contain dimeric antibodies by negative stain electron microscopy (NSEM) (Figure 1B) and size-exclusion chromatography (SEC) (Figure S1A). While dimers were the most prevalent antibody species present, we identified small contributions from higher order IgA species, like tetrameric IgA (Figure S1B).

To confirm passive transfer of 7D9 dIgA into milk, lactating BALB/c dams were infused with 5 mg/kg or 15 mg/kg of 7D9 at 1 to 2 days postpartum and plasma and milk were collected at 1 hr and 1, 3 and 5 days after infusion to assess antibody concentrations (Figure 1C). Peak plasma and milk concentrations of 7D9 antibodies, as measured by a VP6-specific IgA ELISA, were observed 1 hr after infusion in both the 5 mg/kg and 15 mg/kg groups (Figure 1D). To confirm transfer of 7D9 dIgA from milk to suckling pups, a subset of pups were sacrificed 1-day post infusion from both the 5 mg/kg (n=6) and 15 mg/kg (n=6) litters and their ntestinal contents were collected and analyzed for the presence of 7D9. 7D9 was detected in the stomach content of litters born to dams from both 5 mg/kg and 15 mg/kg groups in a dose-dependent manner (Figure 1E). 7D9 antibody levels precipitously dropped 1-day post infusion in both the serum and milk of lactating dams. Low or undetectable levels were observed by day 5 post infusion. This kinetics suggest rapid transfer of 7D9 dIgA to mucosal secretions, including milk. Indeed, 7D9 IgA was also detected in intestinal and rectal content, at low levels in saliva but not in vaginal washes (Figure S2A, B), which suggests pIgR expression differences at different mucosal sites. These data demonstrate systemically-administered dIgA is efficiently transferred from the systemic circulation to milk and other mucosal compartments of mouse dams and subsequently into pup stomach content.

Engineering and recombinant production of a RV-neutralizing mouse-human chimeric dIgA

After demonstrating that systemically-administered 7D9 dIgA can passively transfer from the periphery to milk using our murine lactating mouse model, we aimed to engineer a RV-neutralizing dIgA that could provide protection against RV-induced diarrhea. We constructed a dIgA version of a previously-isolated (Nair et al., 2017) potently-neutralizing RV VP4-specific mAb (mAb#41 or mAb41) by replacing the human IgG1 with the murine IgA constant region and adding the BALB/c J-chain gene on the same open reading frame (Figure 2A). Characterization of the recombinantly produced mAb41 dIgA by ELISA, demonstrated that not all the produced antibody bound to pIgR (Figure 2B), suggesting that in addition to dIgA, non-dimeric or aggregated IgA species were also present. Indeed, NSEM (Figure 3A) and SEC (Figure 3B) revealed multiple IgA species including monomeric and dimeric (Figure 3A) and aggregated (Figure S3) antibodies. We next fractionated the different IgA species based on size and evaluated them for their ability to bind (Figure 3C) and neutralize (Figure 3D) RV. Interestingly, the fraction suspected to be enriched in dIgA (fraction 29-39) had the greatest RV-binding and neutralization capacity compared to the other isolated fractions.

To generate a more homogenous product and skew antibody production towards increased dimer formation, we designed three additional dIgA constructs, where furin cleavage sites were added before the 2A self-cleaving peptides to enhance cleavage, and the J-chain was placed either in the middle (dIgA.2), at the end (dIgA.3) or at the beginning (dIgA.4) of the ORF (Figure 4A). All constructs produced large amounts of total mAb41 IgA antibodies (Figure 4B), however placement of the J-chain gene at the

end of the construct (dIgA.1) resulted in the highest amount of pIgR binding IgA antibodies (Figure 4C).

To address whether modulating the ratio between the J-chain and the heavy and light chains resulted in increased dimer formation, we generated three additional plasmids each separately expressing the heavy [H], the light [L] or the J [J] chain genes and compared dimer production following cells transfection with increasing amounts of J-chain plasmid. Increasing the amount of J-chain DNA resulted in lower levels of pIgR-binding IgA (Figure 4 D), which is concordant with a previous report of recombinant IgA production (Lombana et al., 2019). The 4:4:1, 3:3:1 and 4:4:2 ratio of H:L:J chain plasmids produced the highest level of pIgR-binding dimers (Figure 4D).

Recombinant mAb41 dIgA demonstrates greater RV-binding and neutralization potency than mAb41 monomeric IgA or IgG1 antibodies

To exclude functional contributions from aggregated dimeric/polymeric or monomeric IgA (mIgA) antibodies, recombinantly produced mAb41 dIgA was fractionated by SEC (Figure 5A) and the average molecular weight of 300 kDa was selected as fractionated mAb41 dIgA (f-dIgA mAb41), which is consistent with the expected mass of dIgA at approximately 335 kDa. NSEM demonstrated that the f-dIgA mAb41product contained only dimeric antibodies (Figure 5B)**.** The f-mAb41 dIgA product was then tested for functional capacity in comparison with mIgA mAb41 and IgG mAb41. f-dIgA mAb41 demonstrated greater RV-binding capacity and neutralization activity (AUC=31.9; IC_{90} = 7.1 ng/ml) compared to mIgA (AUC=24.8; IC_{90} = 44.8 ng/ml) or IgG (AUC=19.7; IC_{90} = 33.01 ng/ml) (Figures 5C and 5D). This difference in neutralization activity was even greater when IC_{90} values were normalized for antibody molecular weight, resulting in a

42-fold reduction in IC_{90} value for f-dIgA mAb41 (21.2 pM) compared to mIgA (298.3 pM) and IgG (220.5 pM).

Pharmacokinetics (PK) of intravenous 7D9 dIgA infusion in the blood and milk compartments of lactating BALB/c dams

To determine the optimal dose of dIgA for systemic maternal infusion, we used an Empirical Bayesian estimate of individual PK parameters in both plasma and milk from 7D9 infused dams. Antibody level data were used in simulation for multiple doses including 5 mg/kg (Figure S4A), 10 mg/kg (Figure S4B), and 15 mg/kg (Figure S4C). To estimate the antibody concentrations in serum and milk, 7D9 concentrations were simulated at 24 to 192 hrs in 24-hr intervals. Dosing intervals of 1 to 3 days were explored. Using a 1-day dosing interval, concentrations of 7D9 remained stable up to 8 days after the first dose (Figure S4A). However, with the 2- (Figure S4B) and 3-day (Figure S4C) dosing intervals, 7D9 concentrations dropped by day 2 post-infusion and continued to decrease without an additional dose. The intercompartmental clearance from plasma to milk was 0.11 mL/h and the elimination half-life was 13.55 (6.13 – 18.90) hrs. The observed elimination half-life of 7D9 dIgA is similar to that of dIgA reported in other species (<1 day to ~4 days), including mice and rhesus macaques (Challacombe and Russell, 1979; Lombana et al., 2019)

Maternal passive immunization with systemic mAb41 dIgA protects against RV-induced diarrhea in suckling pups

To determine if passive transfer of mAb41 dIgA in milk results in protection from RV induced diarrhea in suckling neonates, we developed a RV challenge model using lactating 129sv mice dams and their pups. We chose 129sv mice strain as 129sv pups

develop detectable diarrhea after oral inoculation with human RV (Nair et al., 2017). We first confirmed that similarly to BALB/c mice, both fractionated and unfractionated mAb41 dIgA passively transferred into the milk of 129sv mice after IV infusion (Figure S5). In addition to blood and milk, mAb41 dIgA was also detected in vaginal washes and feces, but not in intestinal content (Figure S5). This was different from what we observed in BALB/c mice (Figure S2), suggesting strain-specific differences in pIgR expression resulting in different rates of passive transfer of the two dimeric IgA antibodies. Next, lactating 129sv dams were injected in the tail vein with 5 mg/kg of f-dIgA mAb41 at 4 to 6 days postpartum (Figure 6A). Due to the short half-life of dIgA in milk, as determined by our PK analysis (Figure S4) and to maximize the amount of f-dIgA mAb41 in the gastrointestinal tract of suckling pups at the time of RV inoculation, pups were inoculated with 1×10^6 FFU of RV Wa strain between 1 to 2 hrs post dam injection. Litters born to dams injected with 5 mg/kg mAb41 dIgA had lower incidence of diarrhea (7.1%) upon gentle abdomen palpation (Figure 6B,D) compared to litters born to saline-immunized dams (88%) (Figure 6C,D). Significantly lower RV antigen per gram of intestine was observed in pups born to mAb41 dIgA-immunized mothers compared to pups of saline-injected mothers (Figure 6E). Additionally, mAb41 dIgA was detected in the stomach contents of the suckling pups (Figure 6F), which exhibited RV neutralization capacity at the highest dilution measured (Figure 6G) without compromising viability of the cell monolayer (Figure S6). Thus, mAb41 dIgA passively transferred to suckling pups through the milk of lactating dams to protect against RV-induced diarrhea.

DISCUSSION

Breast milk contains high levels of sIgA that act as the first line of defense against enteric infection in suckling infants (Glass and Stoll, 1989; Ruiz-Palacios et al., 1990; Torres and Cruz, 1993). Despite this, the burden of RV disease in LMIC remains high, likely due to a combination of factors including high pathogen load, malnutrition and decreased vaccine efficacy compared to high income countries (Guerrant et al., 2008; Otero et al., 2020; Velasquez et al., 2018). Neutralizing antibodies against the external RV proteins VP4 and VP7 play a role in protective immunity against RV infection (Clarke and Desselberger, 2015; Desselberger and Huppertz, 2011; Greenberg et al., 1983; Offit and Blavat, 1986). Therefore, enhancing RV-neutralizing sIgA in breast milk is an ideal strategy to provide protection against RV disease in the suckling infant. However, to date, there are no mAb therapies approved or tested for the treatment or prevention of neonatal infection via passive transfer into breast milk in either humans or animal models. In this study, we sought to develop therapeutic strategies that deliver maternal sIgA into breast milk and could enhance protection against RV disease in the suckling neonate.

We first developed a mouse lactation model and demonstrated that a systemically administered a RV non-neutralizing 7D9 dIgA purified from a previously described hybridoma (Greenberg 1996) passively transfers into dams' breast milk and the gastrointestinal tract of suckling pups. We then investigated the half-life of a RV neutralizing mAb41 dIgA. After systemic infusion, the elimination half-life was short [13.55 (6.13 – 18.90) hrs] compared to what is reported for circulating IgG (15-30 days depending on the subclass) (Mankarious et al., 1988) and was consistent with previous

reports (Lombana et al., 2019). Varying amounts of mAb41 dIgA were also detected in the intestinal content, vaginal washes, and saliva. These data suggest that in addition to breast milk, systemically-administered dIgA can traffic to other pIgR-expressing mucosal sites. Dimeric IgA mAb therapeutic strategies that target a particular site, like the mammary gland, will need to consider the biodistribution into other mucosal tissues. Future work should focus on improving dIgA half-life using viral vectors or nucleic acid delivery systems, and on developing strategies to target specific mucosal tissues.

Exploration of the therapeutic potential of neutralizing dIgA *in vivo* has been hampered by the difficulties in production and purification of dIgA at desired antibody quantities (Reinhart and Kunert, 2015; Virdi et al., 2016). We therefore generated several plasmid constructs to optimize the production of a potent RV-neutralizing dIgA (mAb41). We observed that the construct in which the J-chain gene was placed after the heavy and light chain genes produced the highest level of dIgA following recombinant production. This suggests that spatiotemporal production of the IgA heavy, light and J-chain in the cell influences dimerization and therefore, dIgA production. While there are few studies investigating the molecular mechanisms of J-chain protein production and IgA multimerization *in vitro* or *in vivo*, a recent study demonstrated that the B cell chaperone protein MZB1 plays a role (Xiong et al., 2019). Recombinant production of dIgAs in cells expressing MZB1 may improve dimer formation. We also observed that decreasing the amount of J-chain DNA relative to heavy and light chain DNA, resulted in higher levels of dIgA. These results are not surprising, given that each dimer comprises two IgA monomers linked together by a single J-chain and are likely due to an imbalance in the ratio of available heavy and light chains that can dimerize with J-chain. Functional

characterization of the newly generated mAb41 dIgA demonstrated that the dimer had higher neutralization potency compared to both IgA and IgG monomers which may be due to the higher number of available binding sites present on dimers compared to monomers. Isotype-specific mAb protection has been previously demonstrated in both *in vitro* and *in vivo* studies. Mice were better protected from influenza infection in the nasopharynx after systemic administration of anti-influenza polymeric IgA antibodies compared to IgG (Renegar and Small, 1991a, b; Renegar et al., 2004). Interestingly, however recombinantly produced poliovirus-specific antibodies had similar neutralization activity whether they were produced as mIgA, dIgA or IgG (Puligedda et al., 2020) which suggests that isotype-specific differences in functional capacity may be pathogen and even epitope specific.

Finally, using the 129sv mouse model of human RV challenge we showed that a systemically-administered RV-neutralizing dIgA antibody can passively transferred into breast milk and protected suckling neonates from RV-induced diarrhea. Our data support the development of passive immunization strategies with neutralizing dIgA in lactating women to reduce mother-to-child transmission of breast milk-transferred enteric infections including RV, norovirus, and poliovirus, and non-enteric infections like HIV. While passive antibody transfer studies via breast milk have yet to be performed in human infants, oral delivery of recombinant mAbs has been explored. Interestingly, while orally fed palivizumab (anti-RSV IgG1 mAb) was not stable across the infant gastrointestinal tract (Lueangsakulthai et al., 2020a), natural anti-RSV IgG and IgA from breast milk were stable through all phases of simulated infant digestion (Lueangsakulthai et al., 2020b). This demonstrates that delivering pathogen-specific

298 sIgA via breast milk may be a more attractive strategy than oral feeding. The differences
299 in stability between breast milk-derived and recombinant anti-RSV antibodies may be
300 due glycosylation differences. Indeed, recombinant antibodies are differentially
301 glycosylated compared to endogenous antibodies and IgA is more heavily glycosylated
302 than IgG, resulting in altered function (Higel et al., 2016; Langel et al., 2020).

303 The protective transfer strategy is attractive for clinical translation for several reasons:
304 (1) dIgA antibodies directly traffic to mucosal sites, including the mammary gland and
305 passively transfer into breast milk and then to the infant digestive tract as sIgA; (2)
306 dIgA/sIgA may have increased capacity for virus neutralization compared to IgG; (3)
307 breast milk sIgA is more resistant to proteolysis in the stomach and/or gut compared to
308 other isotypes oral delivery of recombinant sIgA in infants; 4) the short-half-life of dIgA
309 may circumvent maternal anti-drug reactions; and (5) dIgA in circulation will traffic to
310 other maternal mucosal sites including the gut, providing dual protection of the
311 maternal-neonatal dyad against enteric infection. Future work could focus on increasing
312 the half-life of dIgA and developing strategies to target specific mucosal tissues.
313 Development of novel strategies that reduce infant mortality against enteric infections is
314 imperative to reach the World Health Organization's goal to end preventable deaths of
315 newborns by 2030. Our results will help guide the development of novel maternal
316 immunization strategies, which may leverage passive transfer of neutralizing dIgA into
317 breastmilk and decrease infant morbidity and mortality against enteric pathogens.

318

319 **METHODS**

Cells and viruses

African Green Monkey kidney epithelial cell line MA104 (CRL-2378.1) was obtained from American Type Culture Collection (ATCC) and cultured in MEM-alpha (Life Technologies) supplemented with 10% fetal bovine serum (FBS), 50 µ/ml of penicillin and 50 µg/ml of streptomycin (Invitrogen). Rotavirus strain A (Wa) (ATCC) was propagated in MA104 cells as previously described (Patton et al., 2009).

Rotavirus quantification

RV was quantified using a fluorescence focus forming assay (Patton et al., 2009). In brief, RV was activated with 10 µg/ml of trypsin for 1 hr in a 37°C water bath. Serially diluted virus was added to confluent MA104 cells and incubated for 1 hr at 37°C. Inoculum was removed and growth medium including DMEM (Life Technologies), 5% FBS, 50 µ/ml of penicillin and 50 µg/ml of streptomycin (Invitrogen) was added. Infected cells were then incubated at 37°C for 12 to 18 hrs. Medium was removed from the plates and fixed with 10% formalin in neutral buffered saline for 20 minutes. Wells were then washed with 2% FBS and cells were permeated with 0.5% Triton-X in PBS for an additional 15 minutes. Wells were washed twice and 7D9 (VP6-specific, murine IgA antibody) was added at 10 µg/ml in 2% FBS as the primary detection antibody for 1 hr at room temperature (RT). Cells were washed twice and an anti-murine IgA antibody conjugated to FITC (1:100; Southern Biotec) was added to wells for 1 hr at RT. Cells were washed four times with wash solution and DRAQ5 nuclear stain (Fisher Scientific) was added to cells at 1:2000 dilution. Cells were washed once with PBS and resuspended in 10 µl of PBS. Infection was quantified in each well by automated cell counting software using a Cellomics Arrayscan VTI HCS instrument at ×10

magnification. Subsequently, the percent of infected cells was determined as $FITC^{+}DRAQ5^{+}$ cells.

7D9 Antibody production

The 7D9 hybridoma line was cultured in ClonaCell™-HY Medium E (STEMCELL Technologies) prior to antibody production. To produce large quantities of 7D9, cells were resuspended in Hybridoma Serum Free Medium (Fisher Scientific) and seeded in the cell compartment of a bioreactor, with Medium E providing nutrients from the medium compartment. Antibody was harvested from the cell supernatant after 5 to 7 days post inoculation and purified using Protein L Sepharose beads (Thermo Fisher Scientific).

Construction of mAb41 plasmids and antibody production

To generate the human-mouse chimeric mAb41 IgA and IgG, we took the variable domain sequences of a previously isolated human anti-RV VP4 specific neutralizing mAb (*i.e.*, mAb#41) (Nair et al., 2017), attached it to the murine IgA and IgG constant regions (accession numbers: AB644393.1, JQ048937.1, KT336476.1, JQ048937.1), respectively, and cloned it into the pcDNA3.1 expression vector. A third plasmid encoding the BALB/c J-chain sequence (accession number: AB664392.1) was also generated. The heavy, light and J chain of mAb41 IgA were also cloned into a single open reading frame, and in different orientations as shown in Figure 4. The 2A self-cleaving peptide technology was used to express both the heavy, light and J chain genes from a single open reading frame. Antibodies were produced by transient transfection of human epithelium kidney 293T Lenti-X cells (Clontech Laboratories,

Mountain View, CA) using the JetPrime transfection kit (Polyplus Transfection Illkirch, France) following the manufacture's recommendations. Different amounts of each plasmid were transfected as shown in Figure 4. Antibodies were harvested from cell supernatants at 4 to 5 days post transfection and purified using CaptureSelect™ LC-lambda (mouse) Affinity Matrix (Thermo Fisher Scientific).

Dimeric IgA characterization and purification

Dimeric antibodies (7D9 and mAb41) were characterized and fractionated by size exclusion chromatography using a Superose 6 10/300 GL on an AKTA liquid chromatography system and concentrated on AmiconUltra 100k spin columns (Millipore).

Negative-stain electron microscopy (NSEM)

Antibodies were diluted to 100 mg/ml final concentration with buffer containing 10 mM NaCl, 20 mM HEPES buffer, pH 7.4, 5% glycerol and 7.5 mM glutaraldehyde. After 5-minute incubation, excess glutaraldehyde was quenched by adding sufficient 1 M Tris stock for a final Tris 75 mM for 5 mins; then samples were stained with 2% uranyl formate. Images were obtained with a Philips 420 electron microscope operated at 120 kV, at 82,000 × magnification and a 4.02 A˚ pixel size. RELION 3.0 (Zivanov et al., 2018) was used for CTF correction, automatic particle picking and 2D class averaging of the single-particle images.

Animals

Timed pregnant BALB/c and 129sv mice were obtained from Charles River laboratories and Taconic Biosciences, respectively. Upon arrival, all mice were maintained in a

pathogen-free animal facility under a standard 12 hr light/12 h dark cycle at RT with access to food and water *ad libitum*. Timed pregnant mice received a supplemental nutritional gel to decrease risk of pup savaging. For IV injections of recombinant dIgA mAbs, animals were restrained using a mouse tail vein restrainer. For mouse milking, dams were separated from their pups for at least 2 hrs to allow milk accumulation while pups were kept warm on a heating pad. Dams were administered 2 IU/kg of oxytocin via intraperitoneal (IP) injection. The mammary area was wiped with sterile alcohol prep pad before manually expressing the teat with thumb and forefinger to gently massage the mammary tissue in an upward motion until a visible bead of milk formed at the base of the teat. A sterile pipet tip was used to gently pull the milk into the tip. All teats were milked two times. Milk was diluted 1:4 with PBS and filtered with 0.22 μm Spin-x centrifugal filters (Costar) at 4°C at 15,000 x g for 30 min. The Spin-x filter separated the lipid portion of the milk from the liquid whey portion, and the liquid whey portion was stored in -20°C. Blood samples were collected from the facial vein (submandibular). The blood was allowed to clot at ambient temperature. Clotted blood samples were maintained at RT and centrifuged for 6,000 RPM for 15 min. The serum was separated from the blood and stored at -20°C.

For RV infection, neonatal 129sv mice (5 days old) were orally gavaged with a minimum of 1×10^6 FFU of RV Wa. Pup stomach contents and intestines were collected and homogenized in 500 μm PBS using a TissueLyzer II (Qiagen) for 5 min at 50 Hz with a stainless steel ball added as a pulverizer. Pulverized stomach content and intestinal tissue were transferred to a new microcentrifuge tube and spun for 10 minutes at 3,000 RPM. Supernatants were collected and then filtered via 0.22-μm Spin-x centrifugal filter

tubes by centrifugation at 18,000 × *g* for 20 mins at 4°C. A protease cocktail (1X) (Fisher Scientific) was added (and samples were stored at -20°C until further analysis.

Biodistribution studies

After IV injection of recombinant mAbs, mice were euthanized via CO_2 asphyxiation. Mice oral and vaginal cavities were immediately washed with 100 µL of PBS. Oral and vaginal washes were centrifuged at 3,000 RPM for 10 mins to pellet any cellular debris. The supernatant was then collected and stored at -20°C. Additionally, intestinal and rectal contents were collected and diluted in 500 µl of PBS. The diluted samples were then filtered via 0.22-µm Spin-x centrifugal filter tubes by centrifugation at 15,000 x g for 30 mins. Protease inhibitors were added (1X) and samples were stored at -20°C until further analysis.

VP6 binding IgA antibody ELISA

Recombinant VP6 protein (head domain; residues 147-339 of full-length VP6) was expressed in *E. coli* and purified through affinity chromatography using a Ni-NTA column and size-exclusion chromatography using a Superdex 200 10/300 GL column as previously described (Aiyegbo et al., 2013). Nunc® Maxisorp™ 384-well plates were coated with 3 µg/ml of recombinant VP6 protein diluted in coating solution concentrate (Seracare) overnight at 4°C. Plates were washed one time (PBS, 0.5% Tween-20) and incubated for 2 hrs with blocking solution (PBS, 4% whey protein, 15% goat serum, 0.5% Tween-20). Antibodies were diluted in blocking solution and added to wells in duplicate for 1 hr. Plates were then washed twice and incubated for 1 hr with an HRP-conjugated, goat anti-mouse IgA antibody (Southern Biotech) at a 1:5000 dilution. After

4 washes, SureBlue Reserve TMB Microwell Peroxidase Substrate (KPL) was added to the wells for 10 mins, and the reaction was stopped by addition of 1% HCl solution. Plates were read at 450 nm. OD values within the linear range of a standard curve were used to interpolate the concentration of VP6-binding IgA antibodies in the transfection products. The standard curve was generated by serial dilutions of 7D9 dIgA.

pIgR binding IgA antibody ELISA

J-chain containing IgA antibodies were measured by pIgR binding ELISA. Nunc® Maxisorp™ 384-well plates were coated with 6 µg/ml of recombinant mouse pIgR protein (R&D Systems) diluted in coating solution concentrate (Seracare) overnight at 4°C. The ELISA assay was completed as described above. OD values within the linear range of a standard curve were used to interpolate the concentration of pIgR-binding IgA antibodies in the transfection products. The standard curve was generated by serial dilutions of 7D9 dIgA.

mAb41 anti-idiotypic antibody ELISA

Nunc® Maxisorp™ 384-well plates were coated with 1 µg/ml of an mAb41 anti-idiotypic antibody (Biogenes GmbH) diluted in coating solution (Seracare) overnight at 4°C. The ELISA assay was completed as previously described above. OD values within the linear range of a standard curve were used to interpolate the concentration of pIgR-binding IgA antibodies in the transfection products. The standard curve was generated by serial dilutions of mAb41 mIgA antibodies.

Rotavirus infected cell binding assay

MA104 cells were seeded into 96-well plates and incubated until confluent (3-4 days) at 37°C and 5% CO_2. RV Wa was thawed at RT and activated with 10 µg/ml of trypsin for 30 mins at 37°C. RV was added to cells at MOI 2 and incubated at 37°C and 5% CO_2 for 20 to 22 hrs. Cells were fixed with 10% neutral buffered formalin for 20 mins. Cells were washed once with wash solution (2% FBS in PBS). To permeate cell membranes, 0.5% Triton-X in PBS was added to cells for 15 mins. Cells were washed twice and 7D9 added to all wells at 10 µg/ml and incubated for 1 hr in the dark at RT. Cells were washed twice with wash solution and an anti-mouse IgA FITC secondary (Abcam) was added at 1:100 dilution and incubated for 1 hr in the dark at RT. Cells were washed four times with wash solution and DRAQ5 nuclear stain (Fisher Scientific) was added to cells at 1:2000 dilution. Cells were washed once with PBS and resuspended in 10 µl of PBS. Infection was quantified in each well by automated cell counting software using a Cellomics Arrayscan VTI HCS instrument at ×10 magnification. Subsequently, the percent infected cells were determined as $FITC^+DRAQ5^+$ cells.

Rotavirus neutralization assay. MA104 cells were seeded into 96-well plates and incubated until confluent (3-4 days) at 37°C and 5% CO_2. RV Wa was thawed at RT and activated with 10 µg/ml of trypsin for 30 mins at 37°C. Serial dilutions of mAbs or homogenized stomach contents were incubated with RV Wa (MOI = 4) in 50 µl for 1.5 hrs at 37°C. The virus/mAb or virus/plasma dilutions were then added in duplicate to wells containing MA104 cells and incubated at 37°C for 20 to 22 hrs. Cells were fixed with 10% neutral buffered formalin for 20 mins. Cells were washed once with wash solution (2% FBS in PBS). To permeate cell membranes, 0.5% Triton-X in PBS was added to cells for 15 minutes. Cells were washed twice and 7D9 added to all wells at 10

476 µg/ml and incubated for one hr in the dark at RT. Cells were washed twice with wash
477 solution and anti-mouse IgA FITC secondary (Abcam) was added at 1:100 dilution and
478 incubated for 1 hr in the dark at RT. Cells were washed four times with wash solution
479 and DRAQ5 nuclear stain (Fisher Scientific) was added to cells at 1:2000 dilution. Cells
480 were washed once with PBS and resuspended in 10 µl of PBS. Infection was quantified
481 in each well by automated cell counting software using a Cellomics Arrayscan VTI HCS
482 instrument at ×10 magnification. Subsequently, the ID_{50} was calculated as the sample
483 dilution that caused a 50% reduction in the number of infected cells compared with wells
484 treated with virus only using the Reed and Muench method.

485 *Rotavirus antigen ELISA.* An EDI fecal rotavirus antigen ELISA kit was used according
486 to the manufacturer's protocol. In brief, 100 µl aliquot of the homogenized intestinal
487 samples were diluted in kit diluent and added in equal volumes to duplicate wells. A set
488 of standards was included (0, 1.9, 5.6, 16.7, 50, 150 and 300 ng/ml). Samples were
489 incubated for 1 hr at RT. Wells were washed 5 times with washing buffer and incubated
490 with 100 µl of tracer antibody for 30 mins at RT. The wells were washed and 100 µl of
491 the antibody substrate was added. Samples were incubated in the dark for up to 15
492 mins and 100 µl of stop solution was added to stop the reaction. The absorbance
493 readings were generated at 450 nm. A standard curve was plotted and the antigen
494 concentration in the samples was calculated from the curve.

495 **Acknowledgements**

496 We thank Bridget Pickle and the Duke's Division of Laboratory Animal Resources staff
497 for expert assistance. We thank Kathy Yarborough, Jaimie Carter, and Dr. Jamie
498 Peacock at the Duke Protein Production Facility in the Duke Human Vaccine Institute

for their assistance in size exclusion chromatography. We thank Dr. So Young Kim in the Functional Genomics Facility for her expertise in the Cellomics Arrayscan VTI HCS instrument. The graphical abstract was created using the BioRender (www.biorender.com). This work was supported by the Bill and Melinda Gates Foundation award OPP1189362 (S.P. and M.B.) and funding from the Translating Duke Health Initiative (P.A.).

Author contributions

S.N.L. contributed to study design, analyzed the data and wrote the manuscript. S.N.L., J.T., J.C., T.T., H.W., C.E.O., L.W., J.C., H.G. performed experiments, including antibodies production, ELISA, neutralization assays and in vivo studies. W.H. and H.C. performed the pharmacokinetics analysis. R.E. and K.M. performed the negative stain electron microscopy. V.S. and P.A. performed size exclusion chromatography and molecular weight determination. M.B. and S.R.P. conceived the study, oversaw the planning and direction of the project including analysis and interpretation of the data and editing of the manuscript. All authors read, revised, and approved the final manuscript.

Conflict of interest

J.E.C. has served as a consultant for Luna Biologics, is a member of the Scientific Advisory Board of Meissa Vaccines and is Founder of IDBiologics. The Crowe laboratory at Vanderbilt University Medical Center has received unrelated sponsored research agreements from Takeda Vaccines, IDBiologics and AstraZeneca. S.R.P. provides individual consulting services to Moderna, Merck, Dynavax, and Pfizer. Merck

520 Vaccines and Moderna have provided grants and contracts for S.R.P. sponsored

521 programs.

REFERENCES

Aiyegbo, M.S., Sapparapu, G., Spiller, B.W., Eli, I.M., Williams, D.R., Kim, R., Lee, D.E., Liu, T., Li, S., Woods, V.L., Jr., *et al.* (2013). Human rotavirus VP6-specific antibodies mediate intracellular neutralization by binding to a quaternary structure in the transcriptional pore. PLoS One *8*, e61101.

Appaiahgari, M.B., Glass, R., Singh, S., Taneja, S., Rongsen-Chandola, T., Bhandari, N., Mishra, S., and Vrati, S. (2014). Transplacental rotavirus IgG interferes with immune response to live oral rotavirus vaccine ORV-116E in Indian infants. Vaccine *32*, 651-656.

Arifeen, S., Black, R.E., Antelman, G., Baqui, A., Caulfield, L., and Becker, S. (2001). Exclusive breastfeeding reduces acute respiratory infection and diarrhea deaths among infants in Dhaka slums. Pediatrics *108*, E67.

Blutt, S.E., Miller, A.D., Salmon, S.L., Metzger, D.W., and Conner, M.E. (2012). IgA is important for clearance and critical for protection from rotavirus infection. Mucosal Immunology *5*, 712-719.

Burke, R.M., Tate, J.E., Kirkwood, C.D., Steele, A.D., and Parashar, U.D. (2019). Current and new rotavirus vaccines. Current opinion in infectious diseases *32*, 435-444.

Burnett, E., Jonesteller, C.L., Tate, J.E., Yen, C., and Parashar, U.D. (2017). Global Impact of Rotavirus Vaccination on Childhood Hospitalizations and Mortality From Diarrhea. The Journal of infectious diseases *215*, 1666-1672.

Burns, J.W., Siadat-Pajouh, M., Krishnaney, A.A., and Greenberg, H.B. (1996). Protective effect of rotavirus VP6-specific IgA monoclonal antibodies that lack neutralizing activity. Science *272*, 104-107.

Challacombe, S.J., and Russell, M.W. (1979). Estimation of the intravascular half-lives of normal rhesus monkey IgG, IgA and IgM. Immunology *36*, 331-338.

Clarke, E., and Desselberger, U. (2015). Correlates of protection against human rotavirus disease and the factors influencing protection in low-income settings. Mucosal Immunology *8*, 1-17.

Corthesy, B. (2013). Multi-Faceted Functions of Secretory IgA at Mucosal Surfaces. Frontiers in Immunology *4*.

De Groot, N., Van Kuik-Romeijn, P., Lee, S.H., and De Boer, H.A. (2000). Increased immunoglobulin A levels in milk by over-expressing the murine polymeric immunoglobulin receptor gene in the mammary gland epithelial cells of transgenic mice. Immunology *101*, 218-224.

Desselberger, U., and Huppertz, H.I. (2011). Immune responses to rotavirus infection and vaccination and associated correlates of protection. J Infect Dis *203*, 188-195.

Desyibelew, H.D., and Dadi, A.F. (2019). Burden and determinants of malnutrition among pregnant women in Africa: A systematic review and meta-analysis. PLoS One *14*, e0221712-e0221712.

Glass, R.I., and Stoll, B.J. (1989). The protective effect of human milk against diarrhea. A review of studies from Bangladesh. Acta Paediatr Scand Suppl *351*, 131-136.

Goldblum, R.M., Ahlstedt, S., Carlsson, B., Hanson, L.A., Jodal, U., Lidin-Janson, G., and Sohl-Akerlund, A. (1975). Antibody-forming cells in human colostrum after oral immunisation. Nature *257*, 797-798.

566 Greenberg, H.B., Valdesuso, J., van Wyke, K., Midthun, K., Walsh, M., McAuliffe, V.,
567 Wyatt, R.G., Kalica, A.R., Flores, J., and Hoshino, Y. (1983). Production and preliminary
568 characterization of monoclonal antibodies directed at two surface proteins of rhesus
569 rotavirus. J Virol *47*, 267-275.
570 Guerrant, R.L., Oriá, R.B., Moore, S.R., Oriá, M.O., and Lima, A.A. (2008). Malnutrition
571 as an enteric infectious disease with long-term effects on child development. Nutr Rev
572 *66*, 487-505.
573 Harika, R., Faber, M., Samuel, F., Kimiywe, J., Mulugeta, A., and Eilander, A. (2017).
574 Micronutrient Status and Dietary Intake of Iron, Vitamin A, Iodine, Folate and Zinc in
575 Women of Reproductive Age and Pregnant Women in Ethiopia, Kenya, Nigeria and
576 South Africa: A Systematic Review of Data from 2005 to 2015. Nutrients *9*.
577 Higel, F., Seidl, A., Sörgel, F., and Friess, W. (2016). N-glycosylation heterogeneity and
578 the influence on structure, function and pharmacokinetics of monoclonal antibodies and
579 Fc fusion proteins. European journal of pharmaceutics and biopharmaceutics : official
580 journal of Arbeitsgemeinschaft fur Pharmazeutische Verfahrenstechnik eV *100*, 94-100.
581 Hurley, W.L., and Theil, P.K. (2011). Perspectives on immunoglobulins in colostrum and
582 milk. Nutrients *3*, 442-474.
583 Jayashree, S., Bhan, M.K., Kumar, R., Bhandari, N., and Sazawal, S. (1988). Protection
584 against neonatal rotavirus infection by breast milk antibodies and trypsin inhibitors. J
585 Med Virol *26*, 333-338.
586 Johansen, F.E., Pekna, M., Norderhaug, I.N., Haneberg, B., Hietala, M.A., Krajci, P.,
587 Betsholtz, C., and Brandtzaeg, P. (1999). Absence of epithelial immunoglobulin A
588 transport, with increased mucosal leakiness, in polymeric immunoglobulin
589 receptor/secretory component-deficient mice. J Exp Med *190*, 915-922.
590 Jonesteller, C.L., Burnett, E., Yen, C., Tate, J.E., and Parashar, U.D. (2017).
591 Effectiveness of Rotavirus Vaccination: A Systematic Review of the First Decade of
592 Global Postlicensure Data, 2006-2016. Clinical infectious diseases : an official
593 publication of the Infectious Diseases Society of America *65*, 840-850.
594 Langel, S.N., Otero, C.E., Martinez, D.R., and Permar, S.R. (2020). Maternal
595 gatekeepers: How maternal antibody Fc characteristics influence passive transfer and
596 infant protection. PLoS pathogens *16*, e1008303-e1008303.
597 Lombana, T.N., Rajan, S., Zorn, J.A., Mandikian, D., Chen, E.C., Estevez, A., Yip, V.,
598 Bravo, D.D., Phung, W., Farahi, F., *et al.* (2019). Production, characterization, and in
599 vivo half-life extension of polymeric IgA molecules in mice. MAbs *11*, 1122-1138.
600 Mankarious, S., Lee, M., Fischer, S., Pyun, K.H., Ochs, H.D., Oxelius, V.A., and
601 Wedgwood, R.J. (1988). The half-lives of IgG subclasses and specific antibodies in
602 patients with primary immunodeficiency who are receiving intravenously administered
603 immunoglobulin. J Lab Clin Med *112*, 634-640.
604 Mantis, N.J., Rol, N., and Corthésy, B. (2011). Secretory IgA's complex roles in
605 immunity and mucosal homeostasis in the gut. Mucosal Immunology *4*, 603-611.
606 Matson, D.O., O'Ryan, M.L., Herrera, I., Pickering, L.K., and Estes, M.K. (1993). Fecal
607 antibody responses to symptomatic and asymptomatic rotavirus infections. J Infect Dis
608 *167*, 577-583.
609 Mwila, K., Chilengi, R., Simuyandi, M., Permar, S.R., and Becker-Dreps, S. (2017).
610 Contribution of Maternal Immunity to Decreased Rotavirus Vaccine Performance in

611 Low- and Middle-Income Countries. Clinical and vaccine immunology : CVI *24*, e00405-
612 00416.
613 Nair, N., Feng, N., Blum, L.K., Sanyal, M., Ding, S., Jiang, B., Sen, A., Morton, J.M., He,
614 X.-S., Robinson, W.H.*, et al.* (2017). VP4- and VP7-specific antibodies mediate
615 heterotypic immunity to rotavirus in humans. Science Translational Medicine *9*,
616 eaam5434.
617 Offit, P.A., and Blavat, G. (1986). Identification of the two rotavirus genes determining
618 neutralization specificities. J Virol *57*, 376-378.
619 Otero, C.E., Langel, S.N., Blasi, M., and Permar, S.R. (2020). Maternal antibody
620 interference contributes to reduced rotavirus vaccine efficacy in developing countries.
621 PLoS Pathog *16*, e1009010.
622 Pabst, O., and Slack, E. (2020). IgA and the intestinal microbiota: the importance of
623 being specific. Mucosal Immunology *13*, 12-21.
624 Puligedda, R.D., Vigdorovich, V., Kouiavskaia, D., Kattala, C.D., Zhao, J.Y., Al-Saleem,
625 F.H., Chumakov, K., Sather, D.N., and Dessain, S.K. (2020). Human IgA Monoclonal
626 Antibodies That Neutralize Poliovirus, Produced by Hybridomas and Recombinant
627 Expression. Antibodies (Basel) *9*.
628 Ray, P.G., Kelkar, S.D., Walimbe, A.M., Biniwale, V., and Mehendale, S. (2007).
629 Rotavirus immunoglobulin levels among Indian mothers of two socio-economic groups
630 and occurrence of rotavirus infections among their infants up to six months. J Med Virol
631 *79*, 341-349.
632 Reinhart, D., and Kunert, R. (2015). Upstream and downstream processing of
633 recombinant IgA. Biotechnol Lett *37*, 241-251.
634 Renegar, K.B., and Small, P.A. (1991a). Immunoglobulin A mediation of murine nasal
635 anti-influenza virus immunity. Journal of Virology *65*, 2146-2148.
636 Renegar, K.B., and Small, P.A. (1991b). Passive transfer of local immunity to influenza
637 virus infection by IgA antibody. The Journal of Immunology *146*, 1972-1978.
638 Renegar, K.B., Small, P.A., Jr., Boykins, L.G., and Wright, P.F. (2004). Role of IgA
639 versus IgG in the control of influenza viral infection in the murine respiratory tract. J
640 Immunol *173*, 1978-1986.
641 Ruiz-Palacios, G.M., Calva, J.J., Pickering, L.K., Lopez-Vidal, Y., Volkow, P.,
642 Pezzarossi, H., and West, M.S. (1990). Protection of breast-fed infants against
643 Campylobacter diarrhea by antibodies in human milk. The Journal of Pediatrics *116*,
644 707-713.
645 Tô, T.L., Ward, L.A., Yuan, L., and Saif, L.J. (1998). Serum and intestinal isotype
646 antibody responses and correlates of protective immunity to human rotavirus in a
647 gnotobiotic pig model of disease. J Gen Virol *79 (Pt 11)*, 2661-2672.
648 Torres, O., and Cruz, J.R. (1993). Protection against Campylobacter diarrhea: role of
649 milk IgA antibodies against bacterial surface antigens. Acta Paediatr *82*, 835-838.
650 Trang, N.V., Braeckman, T., Lernout, T., Hau, V.T., Anh le, T.K., Luan le, T., Van
651 Damme, P., and Anh, D.D. (2014). Prevalence of rotavirus antibodies in breast milk and
652 inhibitory effects to rotavirus vaccines. Hum Vaccin Immunother *10*, 3681-3687.
653 Tuaillon, E., Valea, D., Becquart, P., Al Tabaa, Y., Meda, N., Bollore, K., Van de Perre,
654 P., and Vendrell, J.-P. (2009). Human Milk-Derived B Cells: A Highly Activated Switched
655 Memory Cell Population Primed to Secrete Antibodies. The Journal of Immunology *182*,
656 7155-7162.

Velasquez, D.E., Parashar, U., and Jiang, B. (2018). Decreased performance of live attenuated, oral rotavirus vaccines in low-income settings: causes and contributing factors. Expert Rev Vaccines *17*, 145-161.

Virdi, V., Juarez, P., Boudolf, V., and Depicker, A. (2016). Recombinant IgA production for mucosal passive immunization, advancing beyond the hurdles. Cell Mol Life Sci *73*, 535-545.

Xiong, E., Li, Y., Min, Q., Cui, C., Liu, J., Hong, R., Lai, N., Wang, Y., Sun, J., Matsumoto, R., *et al.* (2019). MZB1 promotes the secretion of J-chain–containing dimeric IgA and is critical for the suppression of gut inflammation. *116*, 13480-13489.

Zivanov, J., Nakane, T., Forsberg, B.O., Kimanius, D., Hagen, W.J., Lindahl, E., and Scheres, S.H. (2018). New tools for automated high-resolution cryo-EM structure determination in RELION-3. eLife *7*.

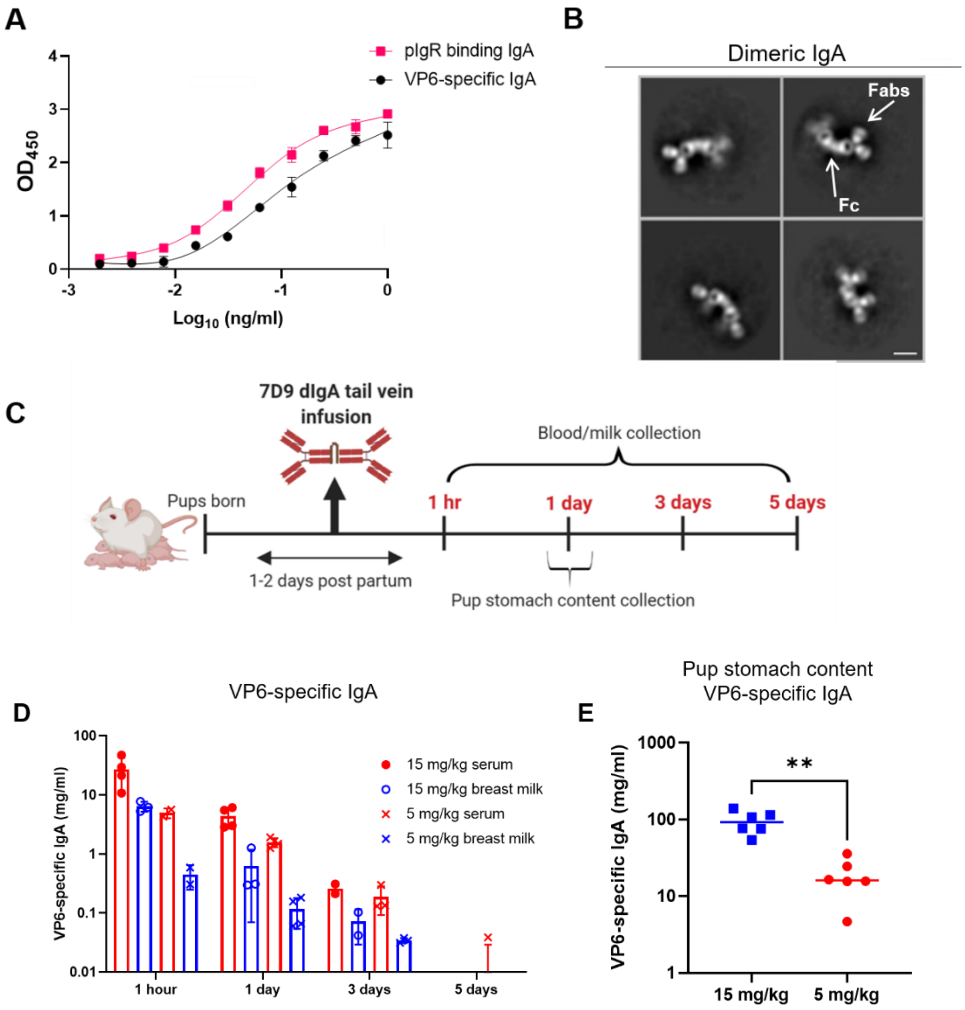

671

672 **Figure 1. Dimeric IgA antibodies administered systemically to lactating mice are**
673 **transferred to milk and the stomach contents of suckling pups**. (A) The rotavirus
674 (RV) VP6-specific, non-neutralizing 7D9 hybridoma derived antibodies bound to RV
675 VP6 (black circles) and polymeric immunoglobulin receptor (pIgR; magenta squares) via
676 ELISA. Data are plotted as mean ± SD of replicates.
677 (B) Negative stain electron microscopy representative images of the hybridoma-purified
678 7D9 dimeric IgA (dIgA) antibodies. The Fab and Fc regions are indicated respectively.
679 Scale bar represents 10 nm. (C) Schematic of tail vein injections of BALB/c lactating

680 dams given 5 mg/kg or 15 mg/kg 7D9 dIgA at 1 to 2 days postpartum. Blood and milk
681 were collected from dams at 1 hr and 1, 3 and 5 days post injection. A subset of pups
682 (n=6) per treatment group were sacrificed at 1-day post injection to collect their stomach
683 content. The schematic was created with Biorender. (D) 7D9 antibodies were detected
684 in blood and milk of injected dams at 1 hr and 1, 3 and 5 days post injection via a RV
685 VP6-specific IgA antibody ELISA. The 5 mg/kg (x) and 15 mg/kg (triangle) treatment
686 groups are indicated for serum (red) and milk (blue). Data are plotted as mean ± SD
687 and represent individual mice. (E) 7D9 antibodies were detected in the stomach content
688 of suckling pups via a RV VP6-specific IgA antibody ELISA in a dose-dependent
689 manner (5 mg/kg = red circles; 15 mg/kg = blue squares). Data are plotted as mean ±
690 SD and represent individual pups. A significant difference between the compared
691 groups (**$p < 0.01$) was determined using a Mann-Whitney U test.
692
693
694
695
696

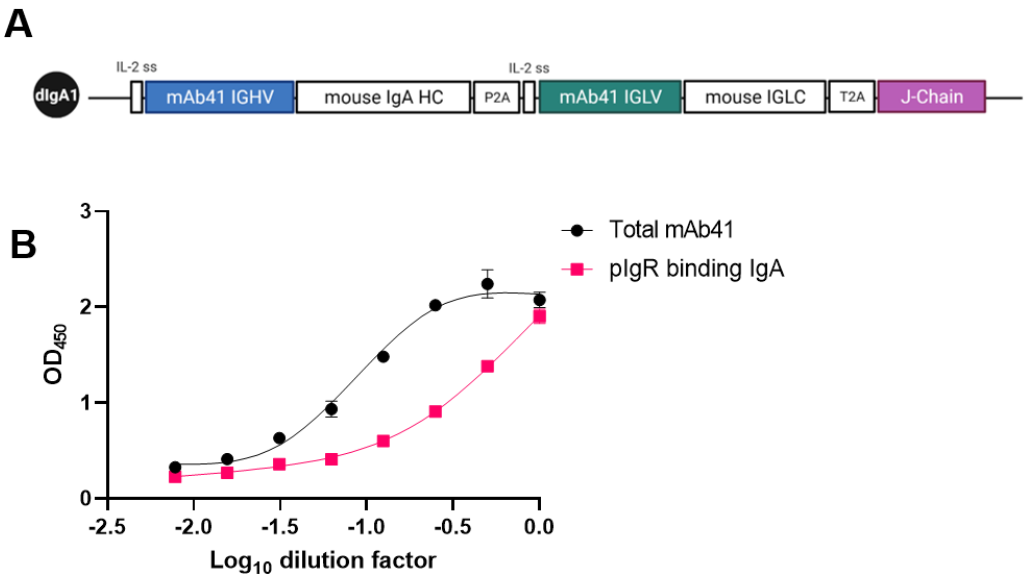

Figure 2. Recombinant production of an RV-neutralizing mouse-human chimeric dIgA antibody. (A) Schematic of the plasmid used to produce the mouse-human chimeric mAb41 dimeric IgA. The mAb41 immuoglobulin heavy chain variable (IGHV) gene (blue box), immunoglobulin light chain variable (IGLV) gene (green box), and the joining chain (J-chain) gene (purple box), are indicated in that order. Schematic created with Biorender. (B) J-chain containing IgA antibodies (mAb 41 = black circles) were detected via a polymeric immunoglobulin receptor (pIgR) binding ELISA. A positive control mAb (magenta squares) was included. Data are plotted as mean ± SD of replicates.

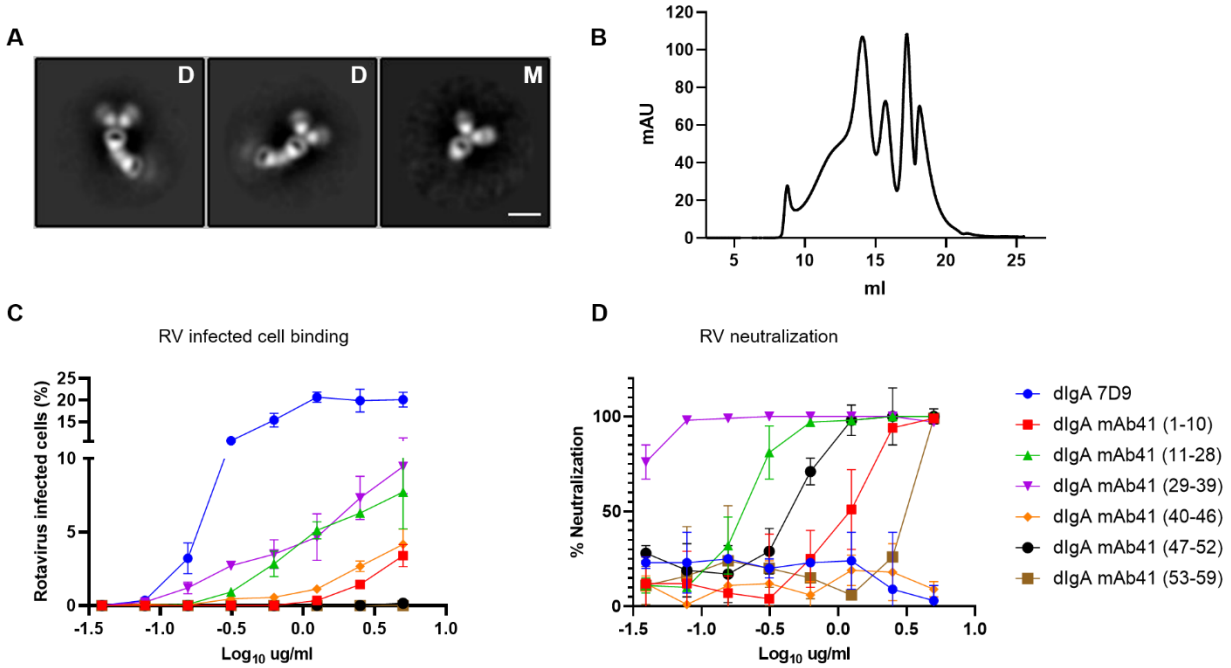

Figure 3. Characterization of recombinant mAb41 IgA antibodies.

(A) Representative negative stain electron microscopy images of purified dimeric (D) and monomeric (M) mAb41 IgA antibodies. (B) Size exclusion chromatography using a Superose 6 10/300 GL revealed multiple different peaks. Each of the peaks were fractionated and the corresponding fractions (1-10, 11-28, 29-39, 40-46, 47-52 and 52-59) functionally characterized by rotavirus (RV)-infected cell binding (C) and neutralization assays (D). RV-infected MA104 cell binding assays revealed that fraction 29-39 bound the strongest to infected cells (C). Similarly, this fraction had the most potent neutralization of RV as determined via RV neutralization assays (D). Based on molecular mass this fraction contains dIgA. The non-neutralizing 7D9 dIgA (blue line) was used as a positive control for binding and a negative control for neutralization. Data are plotted as mean ± SD of replicates.

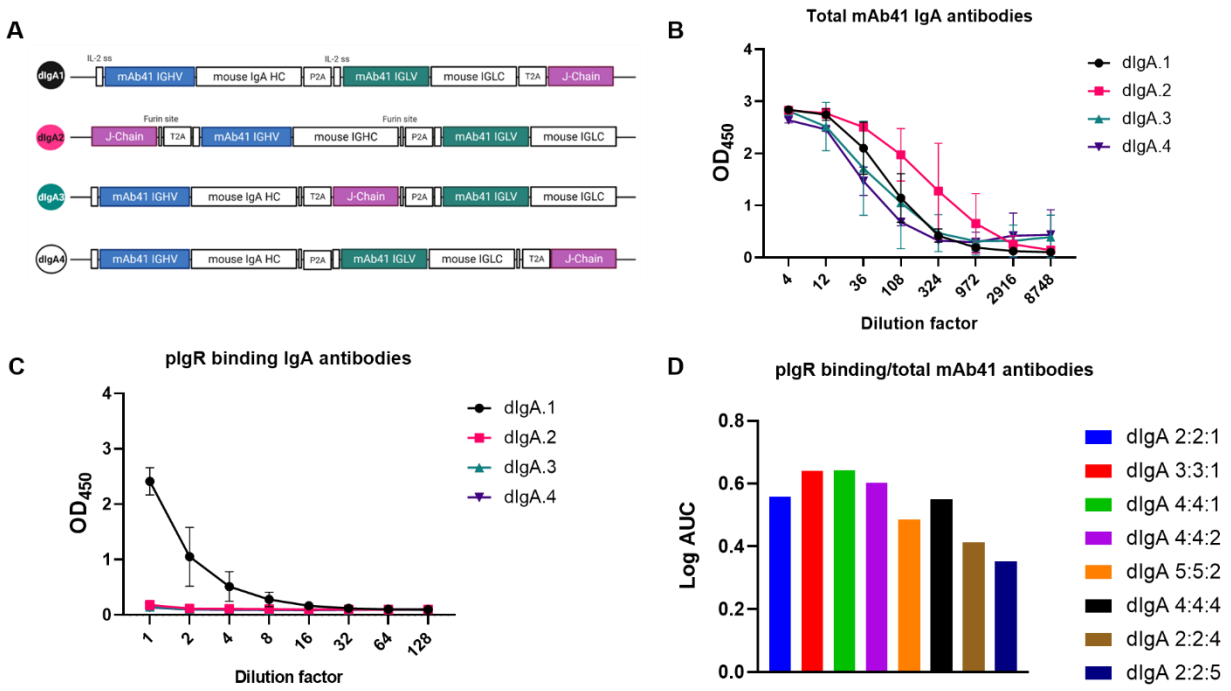

Figure 4. Antibody chains position and ratio impacts the recombinant production of RV-neutralizing mouse-human chimeric mAb41 dimeric IgA. (A) Schematic of the different constructs generated to determine if the position of the J-chain gene in the plasmid cassette impacts dimeric IgA (dIgA) production. Illustration created with Biorender. (B) All constructs produced high amounts of mAb41 IgA. However, placement of the J-chain gene at the end of the plasmid cassette (dIgA.1) resulted in the highest amount of pIgR binding IgA antibodies as determined by ELISA (C). Data are plotted as mean ± SD of experimental duplicates. (D) To determine the optimal ratio of heavy light and J-chain for dimeric IgA production, we co-transfected three separate plasmids each expressing either the heavy (H), the light (L) or the J-chain (J) in varying amounts as depicted on the graph. pIgR IgA antibodies and total mAb41 IgA antibodies were detected via ELISA. Log area under the curve (AUC) was calculated for each co-transfection and graphed as a ratio of pIgR binding IgA antibodies over total mAb41 IgA

antibodies. Greater production of pIgR binding IgA antibodies was achieved when lower amounts of J-chain expressing plasmid were used compared to heavy and light chain plasmids. Data are plotted as mean ± SD of experimental duplicates.

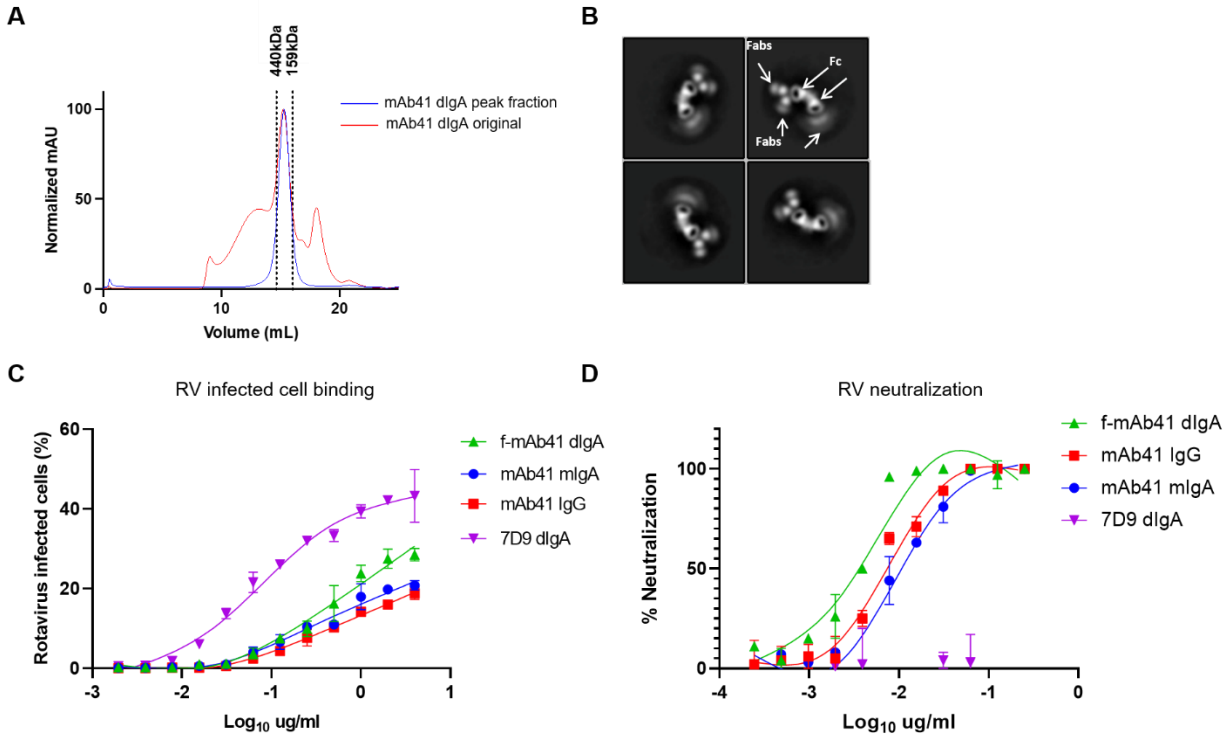

739

740 **Figure 5. Recombinant mAb41 dimeric IgA antibodies demonstrate greater**
741 **rotavirus binding and neutralization potency than mAb41 monomeric IgA or IgG**
742 **antibodies**. (A) Size exclusion chromatography by Superose 6 Increase 10/300 GL
743 column in 1XPBS of mAb41 dimeric IgA (dIgA) antibodies at a flow rate of 0.75 ml/min.
744 Molecular weight markers are listed above the dashed lines at 440kDa and 158kDa,
745 respectively. (B) Negative stain electron microscopy of the purified fraction revealed
746 only the presence of dimeric antibodies. Fab and Fc regions are indicated respectively
747 by white arrows. (C) Fractionated mAb41 dimeric IgA (f-mAb41 dIgA) antibodies bound
748 stronger to RV infected cells compared to mAb41 monomeric IgA (mIgA) or IgG as
749 determined by a RV infected cell binding assay. Data are plotted as mean ± SD of
750 replicates. (D) Fractionated mAb41 dimeric IgA (f-mAb41 dIgA) antibodies more
751 potently neutralized RV compared to mAb41 monomeric IgA (mIgA) or IgG as
752 determined by a RV neutralization assay. Data are plotted as mean ± SD of replicates.

753

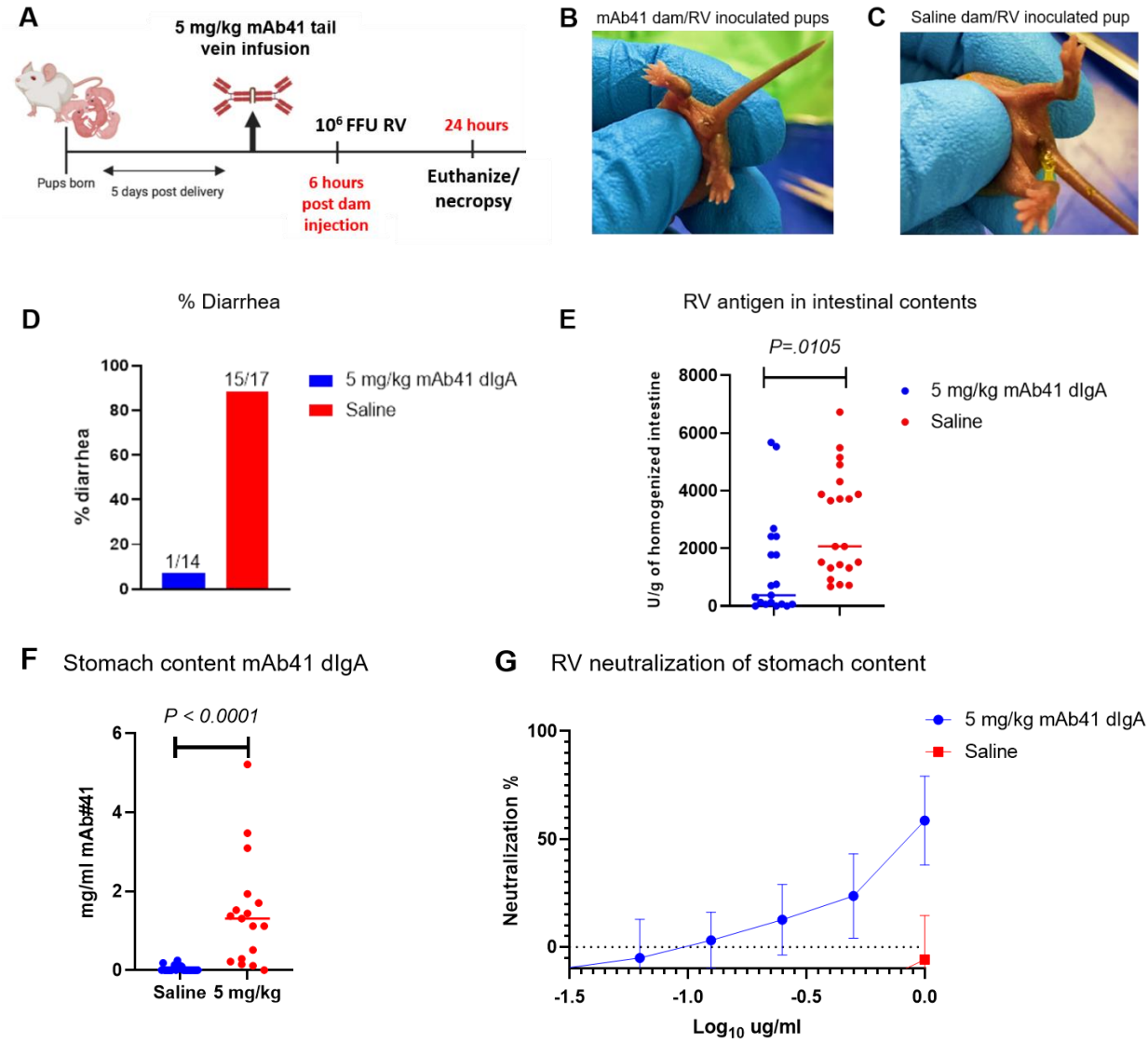

754

755 **Figure 6. Passive maternal immunization with systemic mAb41 dIgA protects**
756 **against rotavirus (RV)-induced diarrhea in suckling pups**. (A) Schematic of tail vein
757 injections of BALB/c lactating dams with 5mg/kg f-dIgA mAb41 antibodies at 5 days
758 postpartum. Pups were orally inoculated with 1×10^6 FFU of RV (Wa strain) at 6 hrs post
759 dam injection and euthanized 24 hrs later. Schematic created with Biorender. (B)
760 Representative image of RV inoculated suckling pups from f-dIgA mAb41 infused dams,

which excreted urine or hard stool upon abdomen gentle palpation. (C) Representative image of RV inoculated suckling pups from saline infused dams, which excreted yellow, liquid and/or stick stool after gentle abdomen palpation. (D) Diarrhea was reported as % of animals with clinical symptoms upon gentle abdomen palpation in each treatment group (5 mg/kg = blue; saline = red). The number of animals with diarrhea out of the total number of animals are reported at the top of each bar graph. (E) RV antigen in homogenized intestinal tissue was detected via a commercial RV antigen binding ELISA. Data are plotted as individual values for each animal and the horizontal bar represents the median units of RV antigen per gram of homogenized intestinal tissue. Significant differences between the compared groups were determined using a Mann-Whitney U test (**$p < 0.05$). (F) mAb41 antibodies were detected in stomach content of suckling pups using an mAb41 anti-idiotypic IgA antibody ELISA. Data are plotted as individual values for each animal and the horizontal bar represents the median ng/ml of mAb41 IgA antibodies. Significant differences between the compared groups were determined using a Mann-Whitney U test (***$p < 0.001$). (G) Stomach content was assessed for rotavirus neutralization at different dilutions and plotted as neutralization % in n=6 pups per treatment group (5 mg/kg = blue; saline = red). Data are plotted as the mean ± SD.